Determine the Anticancer Activity and Mechanism of Overcoming Drug Resistance by $Cu(DDC)_2$ NPs in Prostate Cancers

by

Junwei Wang

A thesis submitted to the Graduate Faculty of
Auburn University
in partial fulfillment of the
requirements for the Degree of
Master of Science

Auburn, Alabama
July 12, 2021

Keywords: anticancer; drug resistance; mechanism; nanoparticles; $Cu(DDC)_2$NPs; prostate cancer

Approved by

Feng Li, Chair, Assistant Professor, Drug Discovery and Development
Robert D. Arnold, Professor, Drug Discovery and Development
Jayachandra Ramapuram, Professor, Drug Discovery and Development

Abstract

Copper diethyldithiocarbamate [$Cu(DDC)_2$] complex formed by disulfiram (DSF) and copper ions is a promising therapeutic agent for cancer treatment. However, the poor aqueous solubility of $Cu(DDC)_2$ limited its clinical application. In our previous studies, we developed a stabilized metal ion ligand complex (SMILE) method to prepare $Cu(DDC)_2$ nanoparticle (NP) as an injectable formulation with high drug concentration and excellent physicochemical properties. Our initial *in vitro* studies also demonstrated its potent anticancer activities. In the current study, we extensively investigated the *in vitro* anticancer activities of $Cu(DDC)_2$ NP and demonstrated that it could kill drug-resistant prostate cancer cells by inducing non-apoptotic cell death. Further, $Cu(DDC)_2$ NP effectively inhibited the tumor growth in an *in vivo* paclitaxel-resistant tumor model. In addition, we also performed studies to explore the mechanism of overcoming drug resistance by $Cu(DDC)_2$ NP. Our results showed that $Cu(DDC)_2$ NP did not affect the P-gp activity or change the level of P-gp proteins. It overcomes drug resistance because it is not a substrate of P-gp. Therefore, the use of $Cu(DDC)_2$ NP will not affect the normal function of P-gp and avoid the toxic side effects associated with P-gp inhibitors. It will be a promising therapeutic agent for treating drug-resistant prostate cancers or other solid tumors.

Acknowledgments

The achievement accomplished in this thesis would not be possible without the help and support from a lot of people to whom I would like to give my sincere appreciation.

I want to thank my advisor, Dr. Feng Li, for his endless support and inspirable guide during my two years of study at Auburn University. His mentor helped me to grow into a stronger researcher. I also want to give my sincere gratitude to my committee members, Dr. Jayachandra Ramapuram and Dr. Robert D. Arnold for their valuable advice and precious time on my academic studies and my thesis. They trained me on how to put knowledge into practice.

I would like to thank my labmates, who are also my dear friends, for their continuous support. All the discussions we had are priceless to me. And finally, I want to greatly appreciate my parents. Their selfless love and unconditional belief in me are the essential support in my life.

Table of Contents

List of Tables

List of Figures

List of Abbreviations

$Cu(DDC)_2$	Copper diethyldithiocarbamate
DSF	Disulfiram
SMILE	Stabilized metal ion ligand complex
NP	Nanoparticle
PCa	Prostate cancer
ADT	Androgen deprivation therapy
CRPC	Castration-resistant prostate cancer
ATP	Adenosine triphosphate
ABC	Adenosine triphosphate binding cassette
MDR	Multidrug resistance
P-gp	P-glycoprotein

1. INTRODUCTION

Cancers

Cancers have a long recorded history in both human and other animals. The oldest case was recorded in Egypt as early as 2700 years ago.[1] Nowadays, cancers are growing out of control. In the United States, one in three persons is affected by cancers. In 2020, an estimated 19.3 million new cancer cases were diagnosed, and half of these cases were dead from the disease in worldwide.[2] There are many types of cancers, and they can start to develop anywhere in the human body in an uncontrolled growth manner. As a basic unit of the human body, normal cells can divide to form new cells to fulfill body needs. When cells are old or damaged, they will die, and the divided new cells can take their place. A genetic change occurred on the cells can interfere with the described orderly process of cell renewal and initiate the formation of cancer cells. Cancer cells can grow uncontrollably because they will survive when they are old or damaged and they will not stop dividing to form new cells even the new cells are not needed.[3] The non-stopping division accelerates the growth of cancer cells. Hematologic (blood) cancer and solid tumor cancers are the two main categories of cancers. Cancers of blood cells are called hematologic cancers, these cancers include leukemia, a cancer of bone marrow and blood; lymphoma, cancer that affected the lymphatic system; and myeloma, a cancer of the plasma cells.[4] Unlike solid tumor cancers, hematologic cancers will not generate tumors. Solid tumor cancers are cancers of body organs or tissues, and solid tumors can form during cancer development. Breast, prostate, and lung cancers are the most common cases of solid tumors.[5] A benign tumor will not invade the surrounding environment, and it usually can be removed without recurrence. Therefore, the benign tumor can be harmless in a big chance unless it is formed in the brain, which could be lethal. In contrast, the malignant tumor is much more dangerous. It is capable to spread or invade the surrounding tissue.

Even worse, some cancer cells can enter into a blood and lymph channel and spread, eventually form tumors at a location that may be distinct from the tumor origin.[6] Due to these properties, tumor cells, especially malignant ones, have severely threatened human health.

Prostate Cancer

Prostate cancer (PCa) is one of the leading cancers in the United States. It was at the first place of estimated new cancer cases and the second place of estimated cancer death in the male in 2020.[7] The prostate gland is part of the male reproductive system. Prostate cancer is a disease that malignant cancer cells in the prostate gland start to grow in an uncontrollable manner. Weak flow of urine and frequent urination are both early sign of prostate cancer. Prostate cancer can be diagnosed by prostate or blood examination tests, and a Gleason score can be assigned to evaluate the stage and the grade of prostate cancer.[8]

Current Treatments for Prostate Cancers

Surgery

Surgery is commonly applied for prostate cancer treatment if the cancer cells have not spread out of the prostate gland. Open prostatectomy and laparoscopic radical prostatectomy are the commonly known surgeries to make the incision and remove the prostate.[9] Open prostatectomy is a more traditional method which showed good effect for prostate cancer removal, and it is still a valid treatment option for patients with a large prostate.[10] Laparoscopic radical prostatectomy was developed later. Compared with open prostatectomy, laparoscopic radical prostatectomy has better recovery, less blood loss, better preservation of the neurovascular bundle, and a better vesicourethral anastomosis. However, the effect of laparoscopic radical prostatectomy is highly

dependent on advanced skills and experience of the surgeon. In addition, the high cost and increased risk of thermal injury to the cavernous nerves make the treatment less desirable.[11] Urinary incontinence and erectile dysfunction are the major possible side effects of radical prostatectomy.[11]

Radiation Therapy

Radiation therapy is another commonly used prostate cancer treatment. It can clean the microscopic tumor cells that still remain after surgery, or it can shrink the tumor before surgery.[12] The radiation can generate electrically charged particles and deposits in the cells of targeted tissues. The high energy radiation causes damages to the DNA of the cancer cells and thus inhibits their proliferation. Eventually, cancer cells can be killed by the deposited energy from radiation.[12] However, not only the abnormal cells, radiation also can damage the healthy cells, which is not desirable although healthy cells are usually capable of repairing themselves and restore their normal function faster than cancer cells.[12]

Cryotherapy

Cancer cryosurgery treatment was developed in England in the 1850s. Cryotherapy is to provide an extremely low temperature to prostate cancers in order to freeze these cancer cells to kill them. Liquid nitrogen is the coldest cryogen that has been currently used. In order to successfully destroy cancer cells in the cryosurgical tissues, the process should be efficiently monitored to reach a lethal temperature as soon as possible, to thaw slowly, and to repeat the freeze-thaw cycle.[13]

Hormone therapy

When the cancer cells have spread too far and cannot be treated using surgery or radiation therapy, hormone therapy or called androgen deprivation therapy (ADT) may be used.[14] ADT showed a potent therapeutic effect in 80% to 90% of patients with advanced PCa. The treatment can suppress the growth of prostate cancer by reducing the level of androgen, a male hormone, which can stimulate the growth of prostate cancer. The lower androgen level can slow down the growth of cancer cells, but it will not cure prostate cancer. Even worse, more than half of the patients become resistant to ADT and form castration-resistant prostate cancer (CRPC), and ADT becomes less effective for prostate cancer treatment.[15]

Chemotherapy

Another way is to use chemotherapy for prostate cancer treatment, especially for treating CRPC.[16] Taxane-based chemotherapies have shown great response for treating CRPC.[17] Taxanes, microtubule stabilizing agents, had demonstrated their capability of G2/M phase disruption and inducing cell apoptosis. Taxanes are the first-line medication for CRPC.[18] Despite the initial therapeutic responses, cancer cells often develop acquired resistance to taxanes, such as docetaxel and paclitaxel.[19] The developed drug resistance will limit the therapeutic efficiency and usually will result in a poor prognosis of patients after the recurrence of tumors.

Drug Resistance in Prostate Cancers

The overexpression of adenosine triphosphate (ATP) binding cassette (ABC) transporters plays an important role in the development of multidrug resistance (MDR) to chemotherapy drugs. P-glycoprotein (P-gp) is a drug efflux transporter overexpressed on cancer cell membranes. It is the

primary cause for the resistance of multiple anticancer medicines, including paclitaxel. The role of P-gp in drug resistance in cancer cells has been explored in previous studies..[20, 21] The P-gp efflux transporter can actively transport anticancer drugs out of the cell, reduces the intracellular drug accumulation, and reduces the efficacy of anticancer drugs. Paclitaxel, or docetaxel, show a high affinity for the P-gp transporters, which causes their reduced therapeutic efficiency on drug-resistant cancer cells. In 2010, cabazitaxel was approved by the US food and drug administration (FDA) to s second line medication to treat taxane- resistance PCa. Several studies indicated that the poor substrate affinity of cabazitaxal for P-transporter make cabazitaxel an effective treatment for taxane-resistant prostate cancers. [22] However, the further elevated P-gp transporters on cancer cell membranes can compromise the efficacy of cabazitaxel and worsen the effect of taxane-based chemotherapy. Alternatively, P-gp inhibitor can be applied to block the P-gp activities and allow drugs to accumulate inside cancer cells. The combination therapy of P-gp inhibitor and chemotherapy drugs has been explored extensively to treat resistant cancers.[23] The challenge is that the application of p-gp inhibitor will also interfere with the normal function of p-gp. For example, p-gp plays an important role in drug metabolism. In addition, P-gp can protect the central nervous system from toxins by effluxing diverse substances out of the brain. The inhibition of p-gp can severely intrude the normal function of the human body. Therefore, the use of P-gp inhibitor for overcoming drug-resistance can induce potential threat to human health. In this case, the development of novel anticancer agents to overcome drug resistance without interfering the normal function of P-gp will greatly benefit patients with taxane-resistant PCa.

Disulfiram

Disulfiram (DSF), has been approved by Food and Drug Administration (FDA) for treating alcohol abuse since 1951. It also showed to be effective against cancers during preclinical studies and has been explored for cancer treatment. The anticancer activity of disulfiram is mainly attributed to its metabolite, diethyldithiocarbamate (DDC). DDC chelates divalent metals and forms complexes with copper (Cu). Copper ions can enhance the antitumor effect of DSF. The primary target is the proteasome/poly-Ub protein degradation pathway.[24, 25] The formed $Cu(DDC)_2$ complex binds to the NPL4 protein, induces NPL4-P97 aggregation, and disables P97-NPL4-UFD1 pathway. The inhibition of poly-Ub protein degradation leads to the accumulation of poly-Ub protein in ER, results in ER stress, and eventually causes cell death. The unresolved ER stress could result in cell death *via* apoptosis and non-apoptotic cell death.[26, 27] Several ongoing clinical trials are testing the DSF/Cu combination for patients with glioblastoma, castration-resistant prostate cancer (CRPC), and breast cancer. These clinical trials and other studies used protocols in which DSF and Cu ions were co-administrated in separated formulations. However, due to the poor *in vivo* stability and rapid degradation of DSF,[24, 28] these co-administration approaches achieved inefficient concentrations of $Cu(DDC)_2$ in tumor tissues, thus significantly reduced their anticancer efficacy and clinical potential.[29] Therefore, the administration of $Cu(DDC)_2$ in a single formulation is a more effective approach to obtain higher active drug concentration in the tumor region and achieves better anticancer efficacy. Although the use of preformed $Cu(DDC)_2$ is a promising strategy to achieve potent anticancer effects, it is challenging to develop a formulation of $Cu(DDC)_2$ because of its poor water solubility.[30, 31]

PEG-PLA

Poly(lactic acid)−Poly(ethylene oxide) (PLA−PEG) micelle has been considered as one of the most promising formulation for anticancer drug delivery. It has been used to prepare a commercially available paclitaxel formulation, Genexol-PM. PEG-PLA contains PEG portion, which has a varying molecular weight between 750 Da and 20 kDa, and PLA, which molecular weight was in range of 2 kDa to 110kDa[32]. The PEG shell can form an energetically favored hydrophilic corona, which not only can stabilize the nanoparticle but also can avoid the protein adsorption and phagocytes, which allows the prolonged circulation of NPs in the bloodstream[33]. At the same time, the PLA can form a hydrophobic central core, which allows the encapsulation of therapeutic drugs that have low water solubility. The application of PEG-PLA would allow a prolonged circulation time for a hydrophobic drug in the blood. [32] Due to its excellent biocompatibility, the use of PEG-PLA for developing drug formulation will have fewer regulatory obstacles.

$Cu(DDC)_2$ NP

As mentioned in the previous sections, $Cu(DDC)_2$ complex has very poor solubility in water. Therefore, it would be important to develop a formulation for $Cu(DDC)_2$ complex for its clinical application. To address this issue, we developed a novel Stabilized Metal Ion Ligand Nanocomplex (SMILE) technology as an innovative method to prepare $Cu(DDC)_2$ NP. PEG-PLA was applied as a stabilizer in this formulation. By mixing the stabilizer solutions containing Cu ion and DDC, respectively, the formed $Cu(DDC)_2$ complex was covered by the water-soluble polymer. Therefore, the water solubility of the self-assembling particle can be enhanced. A high loading efficiency above 90% can be achieved by the SMILE method.[34] In addition, as a nanoparticle, the

$Cu(DDC)_2$ complex will be formulated into a nanoscale particle size. The small size allows the enhanced permeability and retention (EPR) effect. Due to the absence of vasculature supportive tissues, tumor tissues usually have 100 nm to 2 μm leaky pores formed in their structures. The vessels on tumor tissue allow the entrance of nanoparticles due to their small size. Once the nanoparticles enter the tumor tissue, they can be more efficiently inhibit the growth of tumors. This formulation could significantly improve the efficacy of the anticancer reagent. The SMILE technology discovered in our lab allows the nanoparticle formulation to be prepared in an inexpensive and straightforward process. Large scale of production can also be easily obtained. The nanoparticle formulation has already been successfully prepared by a 3D-printed microfluidic device with capabilities for continuous production on a large scale.[35]

In this study, we further explored the efficacy of $Cu(DDC)_2$ against drug-resistant PCa with extensive *in vitro* assays and *in vivo* preclinical tumor models established with drug-resistant PCa cells. We also performed experiments to understand its mechanism of overcoming drug resistance (**Figure 1**). Our hypothesis is that $Cu(DDC)_2$ is not a substrate of P-gp, so it will not be effluxed by P-gp. Therefore, the overexpression of P-gp on drug resistance cancer cells will not affect the intracellular accumulation of $Cu(DDC)_2$, and will not affect its anticancer ability. In addition, $Cu(DDC)_2$ will not interfere with the normal function of P-gp. We performed experiments to test our hypothesis, and the results were discussed in detail as the following.

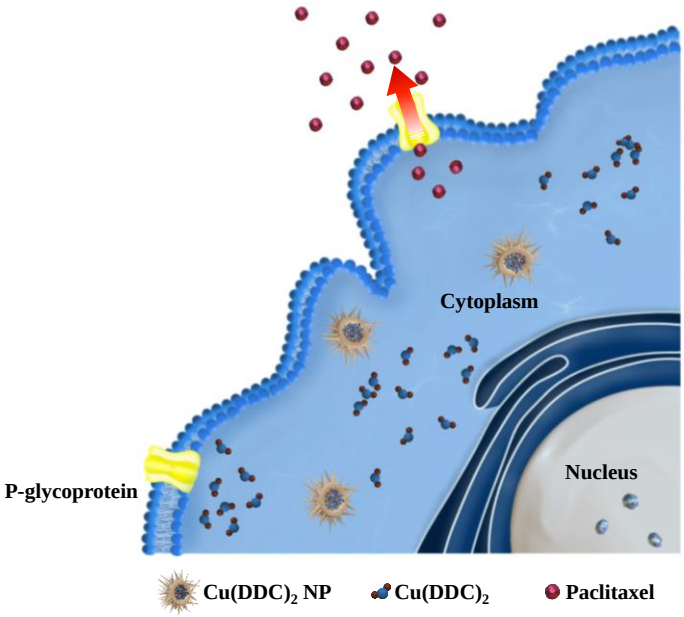

Figure 1. Mechanism of $Cu(DDC)_2$ NP overcome drug resistance

2. MATERIALS AND METHODS

2.1 Materials

PEG_{2K}-$PLA_{1.8K}$ was synthesized with the ring-opening polymerization method as described in our previous study.[36] MDR1/ABCB1 Rabbit mAb (13342S), Anti-rabbit IgG HRP-linked antibody (7074S), β-Actin (4967S) were bought from Cell Signaling. FITC Annexin V Apoptosis Detection Kit was purchased from BioLegend (640914). Alexa Fluor® 647 AffiniPure Goat Anti-Rabbit IgG, Fc fragment specific (131291) was bought from Jackson ImmunoResearch. DAPI fluoromount-G was bought from Electron Microscopy Sciences (180823). Other chemicals and supplies were purchased from VWR International.

PC3, PC3-TXR, DU145, DU145-TXR were provided by Dr. Evan Kellar at the University of Michigan. A549-TXR were provided by Dr. Wei Li at the University of Tennessee. The parental sensitive cells were cultured at 37°C humidified atmosphere using Roswell Park Memorial Institute (RPMI) 1640 medium contained 5% FBS and 1% antibiotic-antimycotic. Resistant cells were cultured with the same medium containing 100nM paclitaxel to maintain the resistance phenotype.

2.2 $Cu(DDC)_2$ NP Preparation and Characterization

$Cu(DDC)_2$ NP were prepared with the SMILE method described in previous publications.[34] Briefly, copper chloride ($CuCl_2$) solution and sodium diethyldithiocarbamatetrihydrate (DDC-Na) solutions were mixed with a vortexer at a 1:2 molar ratio to form $Cu(DDC)_2$ NP with 1% (w/v) PEG_{2K}-$PLA_{1.8K}$ as the stabilizer. The trace amount of aggregation was removed by centrifugation for 10 minutes at 6,700 g. The particle size and zeta potential of NP were measured with Malvern

Nano ZS.[34] The UV-Vis spectrum of $Cu(DDC)_2$ and other control samples were determined with a UV-Vis spectrometer (Nanodrop 2000c). The $Cu(DDC)_2$ concentration was calculated based on the absorption at 435nm with a standard curve established with different concentrations of $Cu(DDC)_2$ dissolved in dimethylformamide (DMF). The yield of nanoparticle production was also calculated with the following equation:

Yield (%) = (Actual $Cu(DDC)_2$ Concentration / Theoretical $Cu(DDC)_2$ Concentration) × 100%

The formation of $Cu(DDC)_2$ in the nanoparticle formulation was also confirmed by HPLC/MS analysis. The analysis was performed with a UPLC system (ACQUITY, Waters Corp. USA) coupled with a quadrupole time-of-flight mass spectrometer (Q-Tof Premier, Waters) with electrospray ionization (ESI) in positive mode using Masslynx software.

2.3 MTT Assay

Cells were seeded in 96-well plates at the density of 5000 cells per well and incubated overnight before the test. Cells were treated with different concentrations of $Cu(DDC)_2$ NP and paclitaxel for 48 hours. The cytotoxicity was determined with the 3-(4,5-dimethylthiazol-2-yl)-2,5-diphenyl tetrazolium bromide (MTT) assay.[34] The cell viability was calculated as the following equation:

Cell viability (%) = $(A_{test}/A_{control}) \times 100\%$.

The IC_{50} was calculated with the Graphpad software. The resistance index was calculated with the following equation:

Resistance index = IC_{50} in resistance cell / IC_{50} in parental sensitive cell.

2.4 Western Blotting Assay

The cell or tissue samples were collected and lysed with the RIPA buffer. The total protein concentration in each sample was determined with a BCA protein assay kit. Proteins in samples were separated with electrophoresis in SDS-PAGE gel (10% w/v) and transferred to a PVDF membrane. The membrane was blocked with 5% w/v non-fat milk in Tris Buffered Saline with Tween 20 (TBST) for one hour at room temperature, incubated with primary antibodies (anti P-gp antibody 1:1000) for 12 hours at 4 ºC, and incubated with secondary antibody (i.e., HRP-linked Anti-rabbit IgG 1:3000). Then, the membrane was imaged after adding ECL western blotting substrate.

2.5 Colony-forming Assay

DU145-TXR cells were seeded in 12-well plates at a density of 1000 cells per well. After incubation for 24 hours, paclitaxel and $Cu(DDC)_2$ NP (500 nM) were added in wells and incubated for 6 hours. Then, the drug-containing medium was replaced with fresh cell culture media and cells were cultured for additional four days. Cell colonies were fixed with 100% methanol and stained with crystal violet.[37]

2.6 Cytotoxicity on Tumor Spheroids

To mimic the real tumor morphology, tumor spheroids were established by culturing DU145-TXR cells in 96-well plates pretreated with agarose gel (1%w/v). The cells were incubated to establish the tumor spheroids for five days. Then, the established spheroids were treated with drugs for 72 hours. The morphology of tumor spheroids was observed under a microscope.

2.7 Annexin V Apoptosis Assay

Cells were seeded in a 12-well plate with a density of 50,000 cells per well. Cells were treated with drugs for 18 hours and then were stained with FITC Annexin V and propidium iodide (PI). The cell apoptosis ($FITC^-/ PI^+$) was analyzed with flow cytometry (BD Accuri C6 plus).

2.8 Caspase 3/7 Activities

DU145-TXR cells were seeded in 96-well plates at a density of 20,000 cells per well. Then, cells were treated with drugs for 18 hours. At the end of treatment, the caspase 3/7 activities in cell lysate were determined with a Caspase Glo 3 reagent (Promega, Madison, WI) and a luminescence microplate reader (Cytation 5 Imaging Reader).[34]

2.9 Xenograft Tumor Model and *In Vivo* Anticancer Efficacy

Drug-resistant tumor model was established by injecting 10^6 DU145-TXR cells in 10-week old male athymic nude mice on the flank.[38] Cells were suspended in 1:1 media and matrigel. When the tumor volume reached around 100 mm^3, mice were randomly divided into three groups and being treated with PBS, paclitaxel micelle (3mg/kg), and $Cu(DDC)_2$ NP (3 mg/kg) through intravenous injection on day 1, 3, 5, 7, and 9. The tumors were measured with a caliper, and tumor volume was calculated with the following formula: 0.5 × long diameter × short $diameter^2$. The body weight of mice was also measured. At the end of the experiment, mice were euthanized, and tumor tissues were collected and weighed.

2.10 P-gp Activities

The intracellular accumulation of calcein-AM (a P-gp substrate) was used to determine P-gp activities.[39] Briefly, cells seeded in 96 well plates were treated with $Cu(DDC)_2$ NP (0.5 μM) or lapatinib (5 μM, a P-gp inhibitor) for 60 minutes prior to the incubation with calcein-AM for 60 minutes. At the end of treatment, intracellular accumulation of calcein-AM was determined with a fluorescence microscope. The fluorescence intensity in the cell lysate was also determined with the Cytation 5 Imaging Reader at the excitation wavelength of 494 nm and emission wavelength of 517 nm. The P-gp activities in 3D cultured tumor spheroids were determined similarly. The 3D tumor provided a platform for further determination on the biological characterization of tumor tissue. The tumor spheroids were also co-stained with DAPI and fluorescence pictures were taken.

2.11 Immunofluorescence Staining

Tumor tissues collected from mice were fixed with 4% paraformaldehyde and cryostat sections were prepared (HM545 NX) for immunofluorescence staining to analyze P-gp on tumor tissues. Briefly, samples were washed with PBS, blocked with 5% milk 0.2% Triton-X 100, incubated with primary antibody (Anti P-gp antibody 1:200), and fluorescence-labeled secondary antibody (1:500). The samples were stained with DAPI and observed with a fluorescence microscope.

2.12 Statistical Analysis

Data were analyzed by GraphPad Prism 8 software. The difference between groups was analyzed with the unpaired t-test. Data was expressed as mean ± SD. Significant difference was defined as * $P<0.05$, ** $P < 0.01$, and *** $P < 0.001$, respectively.

3. RESULTS AND DISCUSSION

3.1 Preparation and Characterization of $Cu(DDC)_2$ NP

The $Cu(DDC)_2$ NP was prepared with the SMILE method developed in our previous studies.[34] The PEG-PLA was selected as a stabilizer. PEG-PLA polymers attached to the surface of *in situ* formed $Cu(DDC)_2$ NP and improved its colloid stability. The PEG block can provide steric protection and reduce opsonization. The PLA block interacts with $Cu(DDC)_2$ core through multiple forces, including coordination bonds and hydrophobic interactions (**Figure 2A**). These strong interactions can efficiently prevent the "strip away" of stabilizers and significantly improve NP stability. The $Cu(DDC)_2$ NP showed a particle size of 46.6 nm, which was slightly larger than PEG-PLA micelles (**Figure2 B and F**). The PEG-PLA micelle and $Cu(DDC)_2$ NP had zeta potential of -9.2±0.7 mV and -46.6±0.3nm, respectively. In addition, the concentration of $Cu(DDC)_2$ was 2 mg/mL with a yield of above 90%. Unlike many drug-loaded NP prepared with conventional methods where drugs were dispersed in the polymer matrix, SMILE method produced NP composed of $Cu(DDC)_2$ complex core surrounded by stabilizers. This unique feature contributed to the high drug loading in our $Cu(DDC)_2$ NP formulation. After mixing DDC-Na with $CuCl_2$ solutions, the color of the mixture turned into dark brown, indicating the formation of $Cu(DDC)_2$ complex, which has a characteristic UV-Vis absorption peak at 435 nm (**Figure 2C**). The formation of $Cu(DDC)_2$ complex in NP formulation was also confirmed with HPLC/MS, which showed a peak of 359 $[M+H]^+$ (**Figure 2E**).

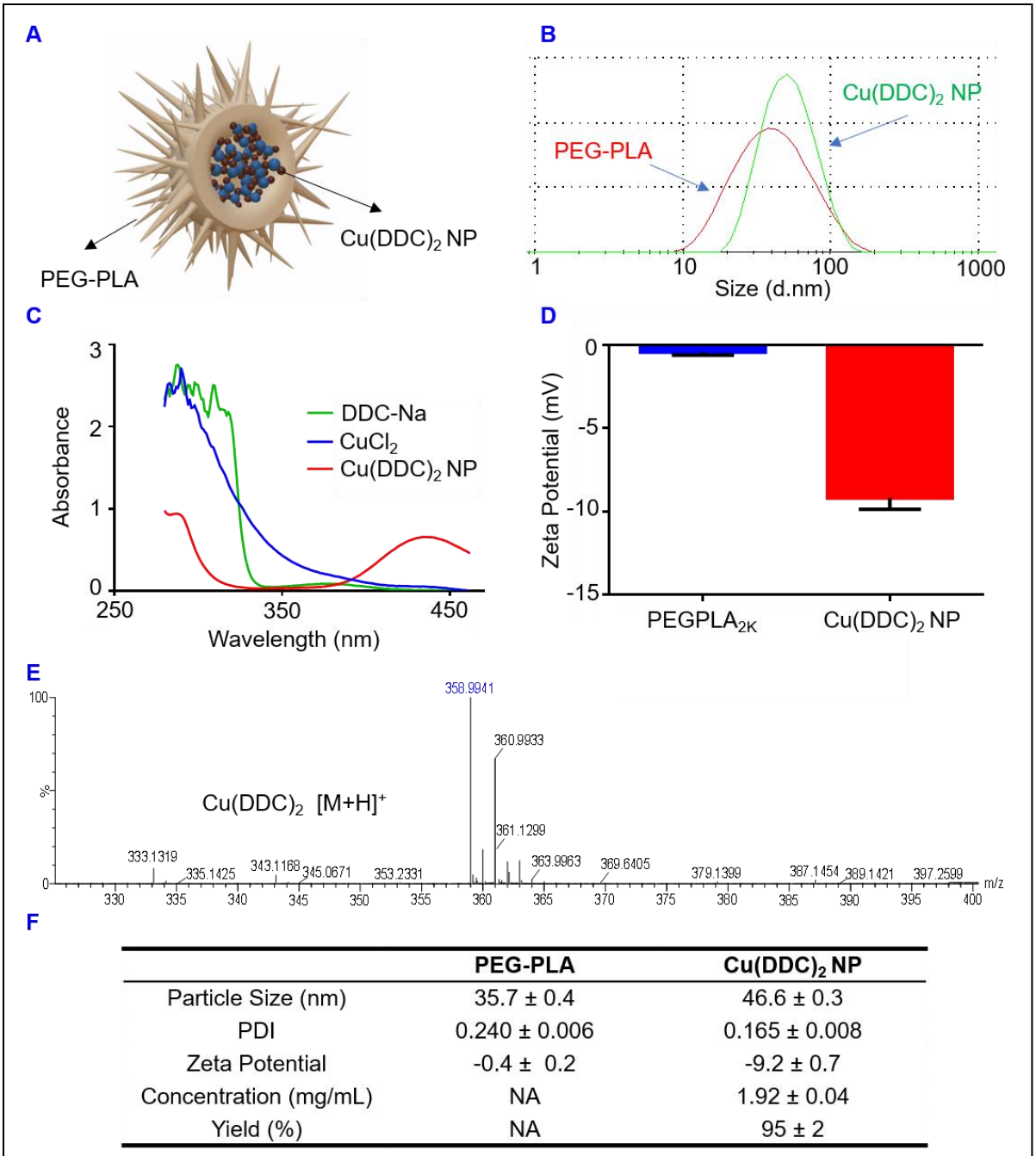

	PEG-PLA	$Cu(DDC)_2$ NP
Particle Size (nm)	35.7 ± 0.4	46.6 ± 0.3
PDI	0.240 ± 0.006	0.165 ± 0.008
Zeta Potential	-0.4 ± 0.2	-9.2 ± 0.7
Concentration (mg/mL)	NA	1.92 ± 0.04
Yield (%)	NA	95 ± 2

Figure 2. Preparation and Characterization of $Cu(DDC)_2$ NP. (A) Schematic representation of $Cu(DDC)_2$ NPs. **(B)** UV-Vis spectrum shows the formation of $Cu(DDC)_2$ with an absorption peak at 435 nm . **(C)** Particle size determined by DLS. **(D)** Zeta potential. **(E)** Mass Spectrum confirm the formation of $Cu(DDC)_2$. **(F)** Table summarizes the properties of $Cu(DDC)_2$ NP. Data are presented as the mean ± SD, n=3.

3.2 *In Vitro* Antitumor Activity Studies

Drug resistance cell lines, PC3-TXR, DU145-TXR and their parent cell lines were chosen to test the anticancer effects of $Cu(DDC)_2$ NP and paclitaxel. Except PCa cells, A549-TXR, a drug resistance lung cancer cell, was also chosen for the test. The resistance cells showed elevated P-gp levels (**Figure 3A**). Since paclitaxel is a known P-gp substrate, the overexpression of P-gp was believed to be a primary reason for developing resistance in these cells.[40, 41] Compared to parental cell lines, the IC_{50} values of paclitaxel was increased dramatically in the drug-resistant cells. The IC_{50} of paclitaxel increased from 7nM in PC3 cell to 533 nM in PC3-TXR cell. The resistance index was 222. Similarly, the IC_{50} of paclitaxel in DU145 and DU145-TXR was 11nM and 2480 nM, respectively. The resistance index was 80 (**Figure 3B-G**). The resistance index of paclitaxel treatment for A549 and A549-TXR reached as high as 118, while the IC_{50} of paclitaxel was 17 nM in A549 and 2046 nM in A549-TXR. These results indicated the development of acquired resistance in PC3-TXR, DU145-TXR and A549-TXR cells. In contrast, the $Cu(DDC)_2$ NP showed similar potent anticancer activities in sensitive PC3, DU145, A549 cells, and resistance ones. No significant change of $Cu(DDC)_2$ NP IC_{50} was observed between PC3, DU-145, A549 and their corresponding paclitaxel resistant cell lines. These initial studies indicated the potential use of $Cu(DDC)_2$ NP to treat drug-resistant cancers.

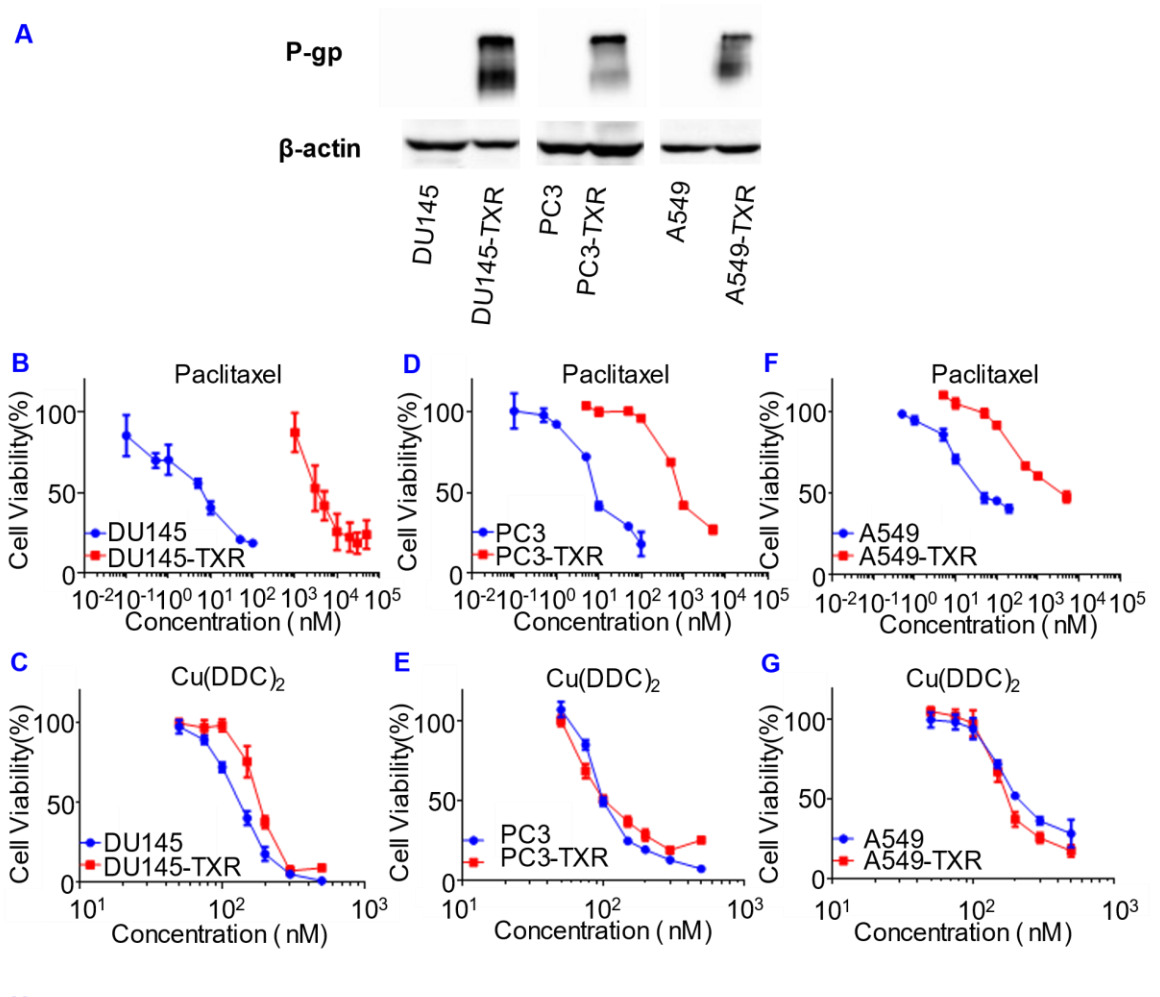

H

Cells	IC_{50} (nM)	
	$Cu(DDC)_2$	Paclitaxel
DU145	147 ± 15	11 ± 2
DU145-TXR	173 ± 11	2480 ± 371
Resistance Index	**1.2**	**222**
PC3	109 ± 10	7 ± 0.6
PC3-TXR	123± 35	533 ± 27
Resistance Index	**1.1**	**80**
A549	155 ± 15	17 ± 9
A549-TXR	153± 15	2046 ± 415
Resistance Index	**1**	**118**

Figure 3. Anticancer effects determined by MTT assay. (A) Western blot shows the over-expression of P-gp in drug resistant cells DU145-TXR & PC3-TXR compared with parental sensitive cells DU145 & PC3. The anticancer effects of $Cu(DDC)_2$ NP **(C)** and Paclitaxel **(B)** on DU145 and DU145-TXR cells was shown. The anticancer effects was also determined on PC3 and PC3-TXR cells treated by $Cu(DDC)_2$ NP **(E)** Paclitaxel **(D)**. The $Cu(DDC)_2$ NP treatment **(G)** and Paclitaxel treatment **(F)** on A549 and A549-TXR were also performed. Data are presented as the mean ± SD, n=4. **(H)** Summary of IC_{50} values. Data are presented as the mean ± SD, n=3.

The anticancer effects of $Cu(DDC)_2$ NP on drug resistance cell lines was further tested with the colony formation assay (**Figure 4A**). Cells were treated with paclitaxel (500 nM) and $Cu(DDC)_2$ NP (500 nM). Due to the acquired resistance, the paclitaxel treatment showed minimal effects on colony formation. However, the treatment of $Cu(DDC)_2$ NP significantly reduced the colony formation when compared with the control or paclitaxel treated group. The anticancer effects of $Cu(DDC)_2$ NP were also tested in 3D cultured tumor spheroids of DU145-TXR cells. After treating tumor spheroids for 72 hours, there was no significant change in tumor spheroids in the control group or paclitaxel (500 nM) treated groups. However, the treatment of $Cu(DDC)_2$ NP showed significant anticancer effects, and the tumor spheroids were disintegrated into small pieces at the end of treatment (**Figure 4B**). The anticancer mechanism of disulfiram and disulfiram/copper combination therapy were investigated in several previous studies. [42-45] Although several studies showed that apoptosis was involved in the DSF/Cu-induced cell death,[46] other studies showed that the activation of caspase was cell-type specific.[24] To confirm the role of apoptosis in $Cu(DDC)_2$ NP induced cell death, we analyzed the $Cu(DDC)_2$ NP treated with DU145-TXR cells with Annexin-V/PI apoptosis assay (**Figure 4C**). Results showed that the percentage of living cells ($FITC^-/PI^-$) in $Cu(DDC)_2$ NP treatment group (52.9 %) was significantly lower than the control group (91.6%). The percentage of dead cells ($FITC^+/PI^+$) in the $Cu(DDC)_2$ NP treatment group (43.5 %) was significantly higher than the control group (7.4 %). However, there was only a minimal number of apoptosis cells ($FITC^+/PI^-$) observed in $Cu(DDC)_2$ NP treatment group (1.8%). These results indicated that the non-apoptotic cell death was induced in DU145-TXR cells treated with $Cu(DDC)_2$ NP. We also determined the caspase 3/7 activities in $Cu(DDC)_2$ NP-treated DU145-TXR cells (**Figure S1**). Despite the significant increase of caspase 3/7 activities in cells treated with staurosporine (positive control), there was no significant increase of caspase 3/7

activities after $Cu(DDC)_2$ NP treatment. Therefore, it is most likely $Cu(DDC)_2$ NP kills cancer cells through non-apoptotic cell death.[34] This properties of $Cu(DDC)_2$ NP will make it a promising drug for treating cancers with defective apoptosis pathways, which is another mechanism for developing resistance in cancer therapy.[47]

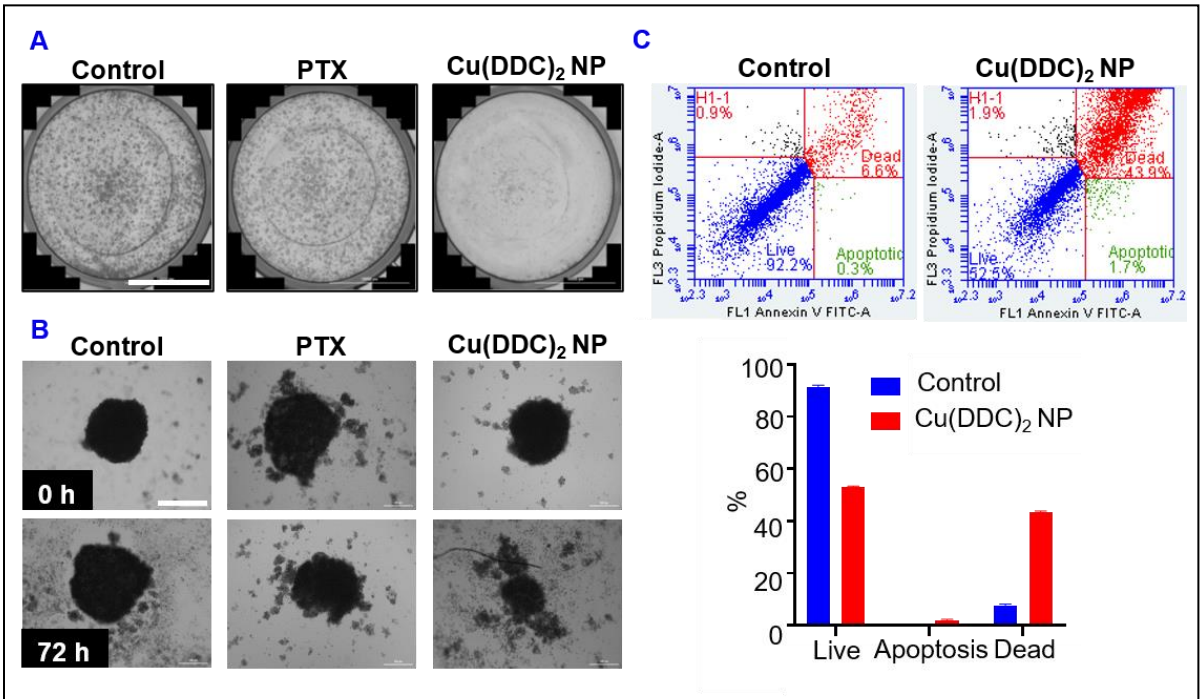

Figure 4. (A) Colony-Forming Assay. DU145-TXR cells formed colonies treated with blank medium, 500nM PTX and 500nM $Cu(DDC)_2$, respectively. Scale bars=10 mm. **(B) Cytotoxicity on Tumor Spheroids.** DU145-TXR cells formed tumor spheroids treated with blank, 500nM PTX and 500nM $Cu(DDC)_2$, respectively, for 72 hours. Scale bars=300μm. **(C) Cell Apoptosis Determined with Flow cytometry**. Cells were treated with control and $Cu(DDC)_2$ NPs (0.5 μM) for 18 hours. Then, cells were analyzed with flow cytometry after staining with FITC-Annexin V and propidium iodide (PI). Representative flow cytometry plots (n=3).

3.3 *In Vivo* Anticancer Efficacy

The *in vivo* anticancer efficacy of $Cu(DDC)_2$ NP was tested with the xenograft tumor model established with DU145-TXR cells on male athymic nude mice. The paclitaxel (3mg/kg) treatment did not show significant inhibition of tumor growth compared with the control group. The poor activity of paclitaxel was expected because a paclitaxel drug-resistant tumor model was used in

the current study. The treatment of $Cu(DDC)_2$ NP (3mg/kg) significantly inhibited the growth of the tumor compared with the saline control group or paclitaxel treated group (**Figure 5A**). The tumor tissue collected at the end of the study also confirmed the anticancer efficacy of $Cu(DDC)_2$ NP (**Figure 5B&C**). The $Cu(DDC)_2$ NP treatment group showed significantly smaller tumor weight and size than the saline control or paclitaxel treated group. Furthermore, no dramatic change of body weight was observed during treatment, indicating the treatment was well tolerated by animals (**Figure 5D**).

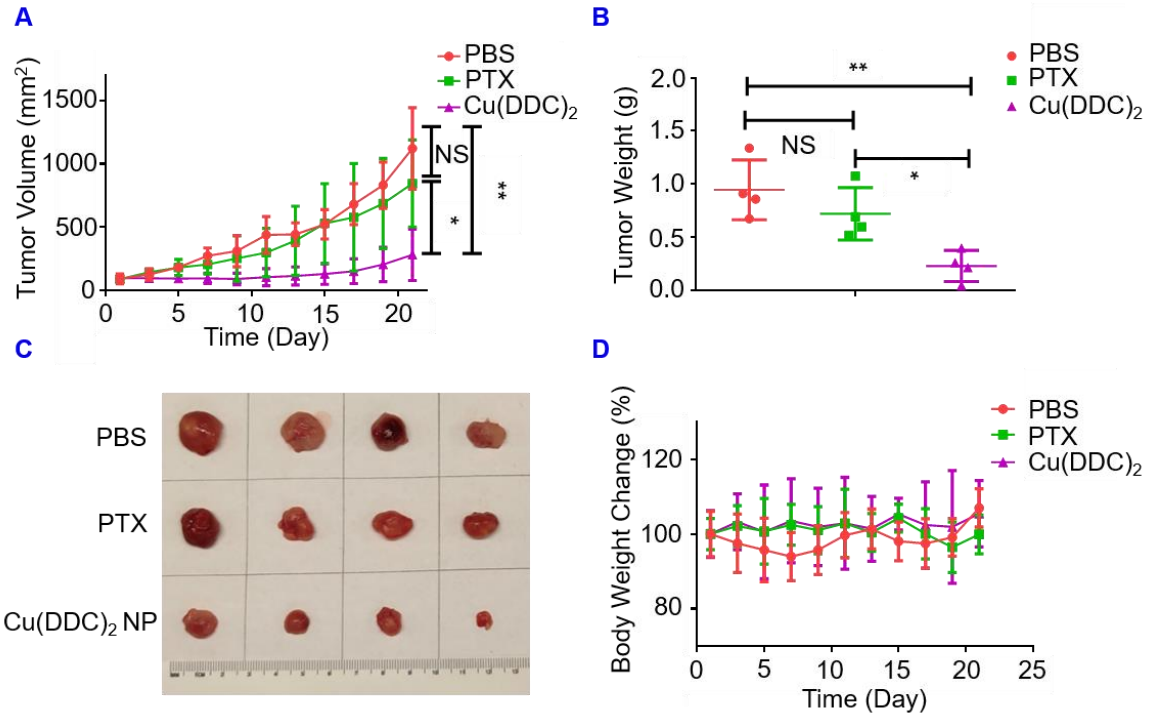

Figure 5. *In vivo* anticancer efficacy with xenograft tumor model established with drug resistant DU145-TXR prostate cancer cells. (A) Tumor growth; **(B)** Tumor Weight; **(C)** Photo of tumor; **(D)** Change of body weight. Data are presented as the mean ± SD, n=4. *, P < 0.05; **, P<0.01.

3.4 Mechanism of Overcoming Drug Resistance

Over-expression of P-gp is often linked to the resistance to chemotherapeutic agents. The DU145-TXR cells showed significantly elevated P-gp, which was the major reason for its resistance to

paclitaxel chemotherapy (**Figure 3A**). The $Cu(DDC)_2$ NP demonstrated potent anticancer efficacy in drug-resistant cells *in vitro* and *in vivo*. We performed several studies to understand the mechanism of overcoming drug resistance by $Cu(DDC)_2$ NP. The effects of $Cu(DDC)_2$ NP treatment on P-gp activities were determined with a calcein-AM based assay. The calcein-AM is a P-gp substrate and can thus be actively transported by P-gp and have minimal intracellular accumulation in cells with overexpressed P-gp.[48] Therefore, the intracellular accumulation of calcein-AM can be used to determine the P-gp activities. **Figure 6A** illustrated the effects of P-gp on intracellular calcein-AM accumulation and the effects of $Cu(DDC)_2$ NP or lapatinib treatment. Due to the over-expression of P-gp in DU145-TXR cells, the intracellular accumulation of calcein-AM was low. DU145-TXR cells treated with $Cu(DDC)_2$ NP showed no significant change of intracellular calcein-AM levels compared with the control group. However, cells treated with lapatinib (P-gp inhibitor control) showed a significant increase of intracellular calcein-AM accumulation (**Figure 6B**). The quantitative results measured based on calcein-AM fluorescence intensity also confirmed the neglectable effects of $Cu(DDC)_2$ NP treatment on the P-gp activities (**Figure 6C**). Although the lapatinib treated group showed significantly increased intracellular fluorescence intensity, no significant change of fluorescence intensity was observed in the $Cu(DDC)_2$ NP treatment group. We performed a similar study in 3D tumor spheroids established with DU145-TXR cells. Both control and $Cu(DDC)_2$ NP treated groups showed minimal intracellular accumulation of calcein-AM, despite the significantly increased accumulation of calcein-AM in tumor spheroids co-treated with lapatinib (**Figure 6D**). These studies indicated that $Cu(DDC)_2$ NP was not an inhibitor of P-gp. We also determine the effects of $Cu(DCC)_2$ NP on the P-gp protein levels of *in vitro* cultured DU145-TXR cells and tumor tissues collected from *in vivo* studies. The western blot analysis showed that both in vitro cultured DU145-TXR cells and

in vivo tumor tissue samples had high levels of P-gp. The treatment $Cu(DDC)_2$ NP did not cause a significant change of P-gp protein levels (**Figure 6F**). The immunofluorescence staining of tumor tissue samples also showed similar results. Both control and $Cu(DDC)_2$ NP treated tumor tissues showed high levels of P-gp. There was no significant difference between these two groups (**Figure 6G**). In our previous study, we co-treated DU145-TXR cells with paclitaxel (a P-gp substrate) + lapatinib combination therapy, which showed significantly more potent anticancer activities than paclitaxel alone.[38] Since paclitaxel and many other chemotherapy drugs are substrates of P-gp, the use of lapatinib (a P-gp inhibitor) can enhance their anticancer activities in drug-resistant cancer cells by inhibiting the P-gp mediated drug efflux.[49] The use of lapatinib will not be able to enhance the anticancer effects of drugs that are not P-gp substrate. As shown in **Figure 6E**, the combination therapy of $Cu(DDC)_2$ plus lapatinib did not show better anticancer activities than $Cu(DDC)_2$ alone as determined with the MTT assay. This study indicated that $Cu(DDC)_2$ NP was not a substrate of P-gp, and the use of P-gp inhibitors will not enhance its activity in drug-resistant cancers.

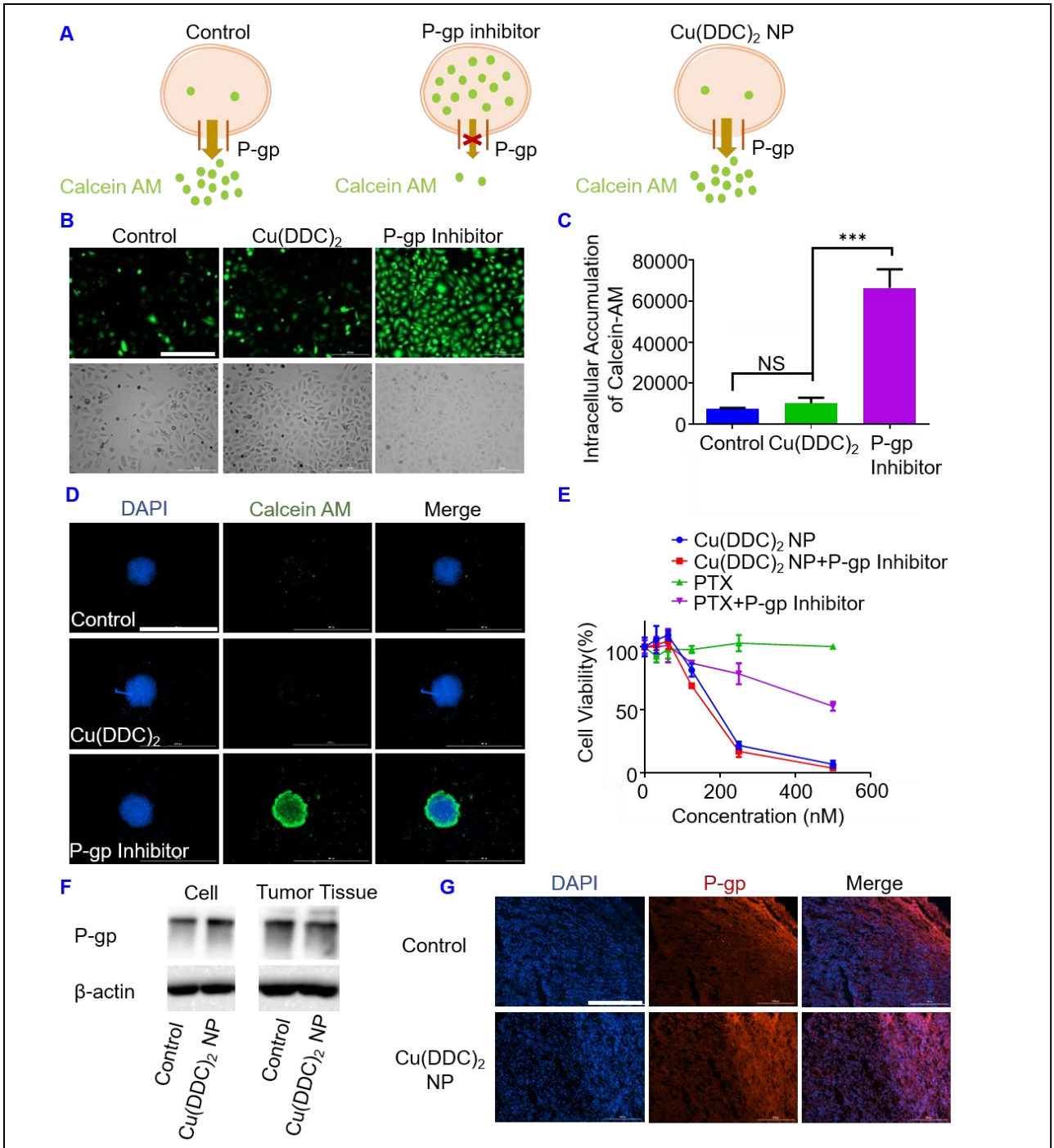

Figure 6. (A). Scheme P-gp transporter pathway under control, P-gp inhibitor and $Cu(DDC)_2$NPs treatment, respectively. **(B) & (C)** Calcein AM accumulation in DU145 TXR under medium, P-gp inhibitor and $Cu(DDC)_2$NPs treatment, respectively. Scale bars=200μm. **(D)** Calcein AM accumulation on 3D tumor sphere**.** Scale bars=1000 μm. **(E)** Cell viability assay of $Cu(DDC)_2$ NP and paclitaxel with or without P-gp inhibitor (1 μM, Lapatinib). Data are presented as the mean ± SD, n=4**. (F)** Effects of $Cu(DDC)_2$ NP treatment on the P-gp protein levels in vitro cultured DU145-TXR cells and in vivo tumor tissues were determined with Western Blot. **(G)** Immunofluorescence of P-gp of DU145TXR tumor tissue. Scale bars=300μm.

It was reported in previous studies that nanoparticle drug formulation could overcome drug resistance and demonstrated more potent anticancer activities than free drug in drug-resistant cells. This might be due to the direct inhibition of P-gp drug transporter by excipients in the formulation. Alternatively, the different intracellular drug transports and release profiles of nanoparticle formulation might also bypass P-gp mediated drug efflux and contribute to the overcome of drug resistance.[50] We compared the *in vitro* anticancer activities of $Cu(DDC)_2$ free drug and $Cu(DDC)_2$ NP formulation. No significant difference was observed, indicating that the ability of $Cu(DDC)_2$ NP to overcome drug resistance was not derived from the NP formulation itself (**Figure S2**).

In summary, our studies indicated that the $Cu(DDC)_2$ NP could effectively treat paclitaxel-resistant cancer with P-gp overexpression. $Cu(DDC)_2$ NP could overcome drug-resistant, because it is not a substrate of P-gp and thus could bypass P-gp mediated drug efflux. The P-gp is broadly distributed in the human body and plays a critical role in drug metabolism. The use of P-gp inhibitors achieved limited clinical success due to the toxicity associate with the inhibition of normal P-gp function. Therefore, the use of $Cu(DDC)_2$ NP will be a promising strategy for overcoming drug resistance without interfering with the normal function of P-gp in the body.

4. CONCLUSION

The development of drug resistance to chemotherapeutic drugs, especially taxanes, reduced the clinical benefits of these drugs. Taxanes showed excellent anticancer activities in PCa. However, their anticancer effects were diminished when drug resistance was developed as prostate cancers evolve.[18] In this study, we investigated the anticancer activity of $Cu(DDC)_2$ NP formulations against paclitaxel-resistant PCa. Both *in vitro* and *in vivo* studies indicated the potent anticancer

activity of this NP formulation. We also performed studies to explore the mechanism of overcoming drug resistance by $Cu(DDC)_2$ NPs. Our results showed that $Cu(DDC)_2$ NP did not affect the P-gp activity or change the level of P-gp proteins. It was able to overcome drug resistance because it was not a substrate of P-gp. This feature of $Cu(DDC)_2$ NP will make it an ideal therapeutic agent for drug-resistant prostate cancers and avoid the potential side effects associated with P-gp inhibition. Although the $Cu(DDC)_2$ NP treatment was mainly studied on drug resistance prostate cancers, we also tested its efficacy on drug-resistance lung cancers. Additional other cancer cell lines can be chosen for further studies to test the potential use of $Cu(DDC)_2$ NP as a broad-spectrum anticancer agent. Since no particular drug resistance on $Cu(DDC)_2$ NP was observed so far, it will be a promising cancer therapy to overcome drug resistance in cancer therapy.

To improve the stability of this formulation, PEG-PLA has been applied as a stabilizer to prepare $Cu(DDC)_2$ NPs. Our previous study demonstrated that the formulation using PEG-PLA as a stabilizer had good stability for short-term storage. Further optimization of the formulation will be needed to facilitate the clinical translation. For example, a lyophilized formulation can further improve the stability of the formulation and make it suitable for long-term storage. The optimization of lyophilized formulation involves the selection of proper excipients (*e.g.*, lyophilization protectors) and lyophilization protocols.

In our studies, the anticancer effect was observed in both *in vitro* and *in vivo* experiments. Despite these proof-of-concept pilot studies, additional studies are required to understand the pharmacokinetics, safety, and efficacy of $Cu(DDC)_2$ NPs. Extensive pharmacokinetics and

biodistribution studies will help us understand the distribution, metabolism and elimination of the drug. The safety of $Cu(DDC)_2$ NPs should also be evaluated. Bodyweight will be measured during the anticancer efficacy study as a sign of acute toxicity. We should also assess the liver toxicity by measuring AST/ALT, ALP levels, kidney toxicity by measuring creatinine levels, heart toxicity by measuring cardiac troponin I and creatine kinase levels, and perform hematology analysis. We can also collect organs (e.g., liver, heart, lung, spleen, and kidneys) and perform histopathology analysis to assess the sign of potential systemic adverse effects. We should use additional tumor models to evaluate the efficacy. The use of orthotopic models, metastatic prostate cancer models, and clinically relevant patient-derived xenograft (PDX) models will provide more valuable information about anticancer efficacy. Furthermore, it will also be interesting to determine whether the $Cu(DDC)_2$ NPs can delay or abrogate the occurrence of acquired resistance.

In summary, we developed $Cu(DDC)_2$ NP as a promising formulation for treating drug-resistant prostate cancers. Additional pre-clinical studies will be needed to develop this formulation and facilitate its clinical translation.

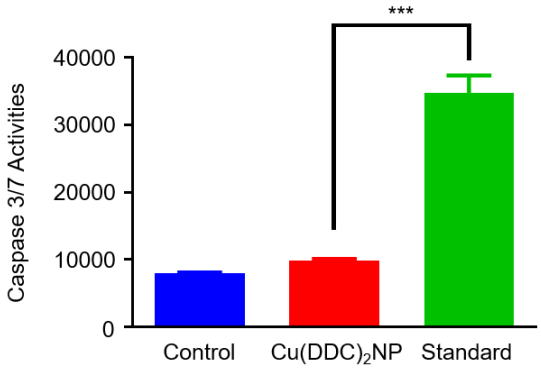

Figure S1. The effects of $Cu(DDC)_2$ NP treatment on Caspase 3/7 activation. Cells were treated with control, $Cu(DDC)_2$ NPs (0.5 μM), and staurosporine (10μM) for 5 hours. Caspase 3/7 activities were determined with Caspase-Glo® 3/7 Assay. Results are the mean ± SD (n = 3). ****, $P < 0.0001$

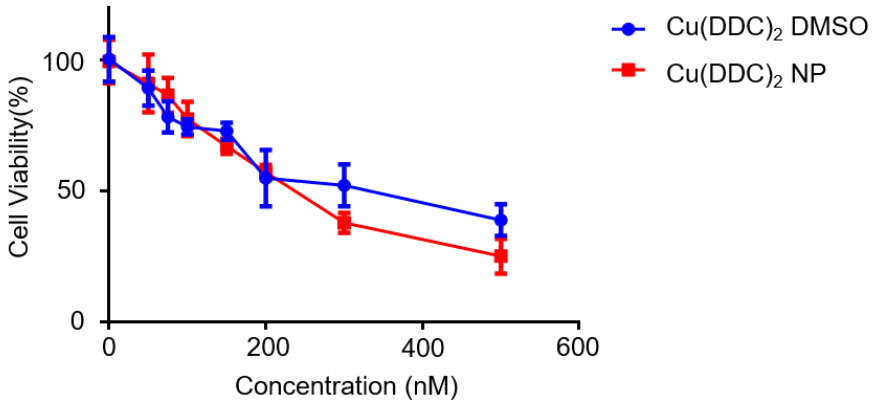

Figure S2. Cell viability of $Cu(DDC)_2$ dissolved in DMSO and Cu(DDC)2 NPs.

References:

1. Faguet, G. B., A brief history of cancer: age‐old milestones underlying our current knowledge database. *International journal of cancer* **2015,** *136* (9), 2022-2036.
2. Sung, H.; Ferlay, J.; Siegel, R. L.; Laversanne, M.; Soerjomataram, I.; Jemal, A.; Bray, F., Global cancer statistics 2020: GLOBOCAN estimates of incidence and mortality worldwide for 36 cancers in 185 countries. *CA: a cancer journal for clinicians* **2021,** *71* (3), 209-249.
3. Mathur, G.; Nain, S.; Sharma, P. K., Cancer: an overview. *Acad. J. Cancer Res* **2015,** *8*, 1.
4. Freireich, E. J.; Keating, M.; Cabanillas, F.; Barlogie, B., The hematologic malignancies: Leukemia, lymphoma, and myeloma. *Cancer* **1984,** *54* (S2), 2741-2750.
5. Nadler, M. B.; Desnoyers, A.; Langelier, D. M.; Amir, E., The effect of exercise on quality of life, fatigue, physical function, and safety in advanced solid tumor cancers: a meta-analysis of randomized control trials. *Journal of pain and symptom management* **2019,** *58* (5), 899-908. e7.
6. Watanabe, S., The metastasizability of tumor cells. *Cancer* **1954,** *7* (2), 215-223.
7. Siegel, R. L.; Miller, K. D.; Jemal, A., Cancer statistics, 2020. *CA: a cancer journal for clinicians* **2020,** *70* (1), 7-30.
8. Borley, N.; Feneley, M. R., Prostate cancer: diagnosis and staging. *Asian journal of andrology* **2009,** *11* (1), 74.
9. Magheli, A.; Gonzalgo, M. L.; Su, L.-M.; Guzzo, T. J.; Netto, G.; Humphreys, E. B.; Han, M.; Partin, A. W.; Pavlovich, C. P., Impact of surgical technique (open vs laparoscopic vs robotic-assisted) on pathological and biochemical outcomes following radical prostatectomy: an analysis using propensity score matching. *BJU international* **2011,** *107* (12), 1956.
10. Suer, E.; Gokce, I.; Yaman, O.; Anafarta, K.; Göğüş, O., Open prostatectomy is still a valid option for large prostates: a high-volume, single-center experience. *Urology* **2008,** *72* (1), 90-94.
11. Lepor, H., Open versus laparoscopic radical prostatectomy. *Reviews in urology* **2005,** *7* (3), 115.
12. Baskar, R.; Lee, K. A.; Yeo, R.; Yeoh, K.-W., Cancer and radiation therapy: current advances and future directions. *International journal of medical sciences* **2012,** *9* (3), 193.
13. Theodorescu, D., Cancer cryotherapy: evolution and biology. *Reviews in urology* **2004,** *6* (Suppl 4), S9.
14. Karantanos, T.; Corn, P. G.; Thompson, T. C., Prostate cancer progression after androgen deprivation therapy: mechanisms of castrate resistance and novel therapeutic approaches. *Oncogene* **2013,** *32* (49), 5501-5511.
15. Hellerstedt, B. A.; Pienta, K. J., The current state of hormonal therapy for prostate cancer. *CA: a cancer journal for clinicians* **2002,** *52* (3), 154-179.
16. Gilligan, T.; Kantoff, P. W., Chemotherapy for prostate cancer. *Urology* **2002,** *60* (3), 94-100.
17. Thadani-Mulero, M.; Portella, L.; Sun, S.; Sung, M.; Matov, A.; Vessella, R. L.; Corey, E.; Nanus, D. M.; Plymate, S. R.; Giannakakou, P. J. C. r., Androgen receptor splice variants determine taxane sensitivity in prostate cancer. **2014,** *74* (8), 2270-2282.
18. Bumbaca, B.; Li, W., Taxane resistance in castration-resistant prostate cancer: mechanisms and therapeutic strategies. *Acta Pharmaceutica Sinica B* **2018,** *8* (4), 518-529.

19. Yin, B.; Zhang, M.; Zeng, Y.; Li, Y.; Zhang, C.; Song, Y., Downregulation of cytokeratin 18 is associated with paclitaxel-resistance and tumor aggressiveness in prostate cancer. *International journal of oncology* **2016,** *48* (4), 1730-1736.
20. Machioka, K.; Izumi, K.; Kadono, Y.; Iwamoto, H.; Naito, R.; Makino, T.; Kadomoto, S.; Natsagdorj, A.; Keller, E. T.; Zhang, J. J. O., Establishment and characterization of two cabazitaxel-resistant prostate cancer cell lines. **2018,** *9* (22), 16185.
21. Xue, X.; Liang, X.-J. J. C. j. o. c., Overcoming drug efflux-based multidrug resistance in cancer with nanotechnology. **2012,** *31* (2), 100.
22. Machioka, K.; Izumi, K.; Kadono, Y.; Iwamoto, H.; Naito, R.; Makino, T.; Kadomoto, S.; Natsagdorj, A.; Keller, E. T.; Zhang, J., Establishment and characterization of two cabazitaxel-resistant prostate cancer cell lines. *Oncotarget* **2018,** *9* (22), 16185.
23. Ma, S.-l.; Hu, Y.-p.; Wang, F.; Huang, Z.-c.; Chen, Y.-f.; Wang, X.-k.; Fu, L.-w., Lapatinib antagonizes multidrug resistance-associated protein 1-mediated multidrug resistance by inhibiting its transport function. *Molecular Medicine* **2014,** *20* (1), 390-399.
24. Skrott, Z.; Mistrik, M.; Andersen, K. K.; Friis, S.; Majera, D.; Gursky, J.; Ozdian, T.; Bartkova, J.; Turi, Z.; Moudry, P.; Kraus, M.; Michalova, M.; Vaclavkova, J.; Dzubak, P.; Vrobel, I.; Pouckova, P.; Sedlacek, J.; Miklovicova, A.; Kutt, A.; Li, J.; Mattova, J.; Driessen, C.; Dou, Q. P.; Olsen, J.; Hajduch, M.; Cvek, B.; Deshaies, R. J.; Bartek, J., Alcohol-abuse drug disulfiram targets cancer via p97 segregase adaptor NPL4. *Nature* **2017,** *552* (7684), 194-199.
25. Bruning, A.; Kast, R. E., Oxidizing to death: disulfiram for cancer cell killing. *Cell Cycle* **2014,** *13* (10), 1513-4.
26. Breckenridge, D. G.; Germain, M.; Mathai, J. P.; Nguyen, M.; Shore, G. C., Regulation of apoptosis by endoplasmic reticulum pathways. *Oncogene* **2003,** *22*, 8608.
27. Skrott, Z.; Mistrik, M.; Andersen, K. K.; Friis, S.; Majera, D.; Gursky, J.; Ozdian, T.; Bartkova, J.; Turi, Z.; Moudry, P. J. N., Alcohol-abuse drug disulfiram targets cancer via p97 segregase adaptor NPL4. **2017,** *552* (7684), 194-199.
28. Wang, Z.; Tan, J.; McConville, C.; Kannappan, V.; Tawari, P. E.; Brown, J.; Ding, J.; Armesilla, A. L.; Irache, J. M.; Mei, Q. B.; Tan, Y.; Liu, Y.; Jiang, W.; Bian, X. W.; Wang, W., Poly lactic-co-glycolic acid controlled delivery of disulfiram to target liver cancer stem-like cells. *Nanomedicine* **2017,** *13* (2), 641-657.
29. McMahon, A.; Chen, W.; Li, F., Old wine in new bottles: Advanced drug delivery systems for disulfiram-based cancer therapy. *Journal of Controlled Release* **2020,** *319*, 352-359.
30. Zhao, P.; Yin, W.; Wu, A.; Tang, Y.; Wang, J.; Pan, Z.; Lin, T.; Zhang, M.; Chen, B.; Duan, Y.; Huang, Y., Dual-Targeting to Cancer Cells and M2 Macrophages via Biomimetic Delivery of Mannosylated Albumin Nanoparticles for Drug-Resistant Cancer Therapy. *Advanced Functional Materials* **2017,** *27* (44), 1700403-n/a.
31. Wehbe, M.; Anantha, M.; Shi, M.; Leung, A. W.; Dragowska, W. H.; Sanche, L.; Bally, M. B., Development and optimization of an injectable formulation of copper diethyldithiocarbamate, an active anticancer agent. *Int J Nanomedicine* **2017,** *12*, 4129-4146.
32. Heald, C.; Stolnik, S.; Kujawinski, K.; De Matteis, C.; Garnett, M.; Illum, L.; Davis, S.; Purkiss, S.; Barlow, R.; Gellert, P., Poly (lactic acid)− poly (ethylene oxide)(PLA− PEG) nanoparticles: NMR studies of the central solidlike PLA core and the liquid PEG corona. *Langmuir* **2002,** *18* (9), 3669-3675.
33. Wang, J.; Li, S.; Han, Y.; Guan, J.; Chung, S.; Wang, C.; Li, D., Poly (ethylene glycol)–polylactide micelles for cancer therapy. *Frontiers in pharmacology* **2018,** *9*, 202.

34. Chen, W.; Yang, W.; Chen, P.; Huang, Y.; Li, F. J. A. a. m.; interfaces, Disulfiram copper nanoparticles prepared with a stabilized metal ion ligand complex method for treating drug-resistant prostate cancers. **2018,** *10* (48), 41118-41128.
35. Chang, Y.; Jiang, J.; Chen, W.; Yang, W.; Chen, L.; Chen, P.; Shen, J.; Qian, S.; Zhou, T.; Wu, L., Biomimetic metal-organic nanoparticles prepared with a 3D-printed microfluidic device as a novel formulation for disulfiram-based therapy against breast cancer. *Applied Materials Today* **2020,** *18*, 100492.
36. Li, F.; Danquah, M.; Mahato, R. I., Synthesis and Characterization of Amphiphilic Lipopolymers for Micellar Drug Delivery. *Biomacromolecules* **2010,** *11* (10), 2610-2620.
37. Crowley, L. C.; Christensen, M. E.; Waterhouse, N. J., Measuring survival of adherent cells with the colony-forming assay. *Cold Spring Harbor Protocols* **2016,** *2016* (8), pdb. prot087171.
38. Li, F.; Danquah, M.; Singh, S.; Wu, H.; Mahato, R. I., Paclitaxel-and lapatinib-loaded lipopolymer micelles overcome multidrug resistance in prostate cancer. *Drug delivery and translational research* **2011,** *1* (6), 420-428.
39. Zaja, R.; Klobučar, R. S.; Smital, T. J. A. t., Detection and functional characterization of Pgp1 (ABCB1) and MRP3 (ABCC3) efflux transporters in the PLHC-1 fish hepatoma cell line. **2007,** *81* (4), 365-376.
40. Takeda, M.; Mizokami, A.; Mamiya, K.; Li, Y. Q.; Zhang, J.; Keller, E. T.; Namiki, M., The establishment of two paclitaxel‐resistant prostate cancer cell lines and the mechanisms of paclitaxel resistance with two cell lines. *The Prostate* **2007,** *67* (9), 955-967.
41. Ambudkar, S. V.; Dey, S.; Hrycyna, C. A.; Ramachandra, M.; Pastan, I.; Gottesman, M. M., Biochemical, cellular, and pharmacological aspects of the multidrug transporter. *Annual review of pharmacology and toxicology* **1999,** *39* (1), 361-398.
42. Skrott, Z.; Cvek, B., Diethyldithiocarbamate complex with copper: the mechanism of action in cancer cells. *Mini Rev Med Chem* **2012,** *12* (12), 1184-92.
43. Wang, N. N.; Wang, L. H.; Li, Y.; Fu, S. Y.; Xue, X.; Jia, L. N.; Yuan, X. Z.; Wang, Y. T.; Tang, X.; Yang, J. Y.; Wu, C. F., Targeting ALDH2 with disulfiram/copper reverses the resistance of cancer cells to microtubule inhibitors. *Exp Cell Res* **2018,** *362* (1), 72-82.
44. Denoyer, D.; Masaldan, S.; La Fontaine, S.; Cater, M. A., Targeting copper in cancer therapy: 'Copper That Cancer'. *Metallomics* **2015,** *7* (11), 1459-1476.
45. Skrott, Z.; Majera, D.; Gursky, J.; Buchtova, T.; Hajduch, M.; Mistrik, M.; Bartek, J., Disulfiram's anti-cancer activity reflects targeting NPL4, not inhibition of aldehyde dehydrogenase. *Oncogene* **2019,** *38* (40), 6711-6722.
46. Yang, Y.; Zhang, K.; Wang, Y.; Li, M.; Sun, X.; Liang, Z.; Wang, L.; Chen, L.; Yang, H.; Zhu, L., Disulfiram chelated with copper promotes apoptosis in human breast cancer cells by impairing the mitochondria functions. *Scanning* **2016,** *38* (6), 825-836.
47. Li, F.; Mahato, R. I., MicroRNAs and drug resistance in prostate cancers. *Molecular pharmaceutics* **2014,** *11* (8), 2539-2552.
48. Chai, A. B.; Hartz, A.; Gao, X.; Yang, A.; Callaghan, R.; Gelissen, I. C., New Evidence for P-gp-Mediated Export of Amyloid-β PEPTIDES in Molecular, Blood-Brain Barrier and Neuronal Models. *International Journal of Molecular Sciences* **2021,** *22* (1), 246.
49. Wang, H.; Li, F.; Du, C.; Wang, H.; Mahato, R. I.; Huang, Y., Doxorubicin and lapatinib combination nanomedicine for treating resistant breast cancer. *Molecular pharmaceutics* **2014,** *11* (8), 2600-2611.

50. Dong, X.; Mumper, R. J., Nanomedicinal strategies to treat multidrug-resistant tumors: current progress. *Nanomedicine* **2010,** *5* (4), 597-615.